

SUPPLEMENTARY FILE

Butyrate reduces appetite and activates brown adipose tissue via the gut-brain neural circuit

Zhuang Li^{1,2}, Chun-Xia Yi³, Saeed Katiraei⁵, Sander Kooijman^{1,2}, Enchen Zhou^{1,2}, Chih Kit Chung¹, Yuanqing Gao³, José K. van den Heuvel^{1,2}, Onno C. Meijer^{1,2}, Jimmy F.P. Berbée^{1,2}, Marieke Heijink⁴, Martin Giera⁴, Ko Willems van Dijk^{2,5}, Albert K. Groen^{6,7}, Patrick C.N. Rensen^{1,2}, Yanan Wang^{1,2,7}

¹Dept. Medicine, Div. Endocrinology, Leiden University Medical Center, Leiden, The Netherlands; ²Eindhoven Laboratory for Experimental Vascular Medicine, Leiden University Medical Center, Leiden, The Netherlands; ³Dept. Endocrinology and Metabolism, Academic Medical Center, University of Amsterdam, Amsterdam, The Netherlands; ⁴Center for Proteomics and Metabolomics, Leiden University Medical Center, Leiden, The Netherlands ⁵Dept. Human Genetics, Leiden University Medical Center, Leiden, The Netherlands; ⁶Amsterdam Diabetes Center, Dept. Vascular Medicine, Academic Medical Center, University of Amsterdam, Amsterdam, The Netherlands; ⁷Dept. Pediatrics, University of Groningen, Groningen, The Netherlands.

SUPPLEMENTARY MATERIALS AND METHODS

Appetite test and brain histology

After overnight fasting (7pm-8am), mice were randomized based on body weight and received sodium butyrate or vehicle by intra-gastric gavage (6 M, 0.15 mL per mouse) or intravenous injection (15 mM or 150 mM, 0.1 mL per mouse). Food intake per se was measured during the next 24 hours.

In a second experiment, 1 hour after intra-gastric gavage of sodium butyrate or vehicle, mouse brains were collected for histological analysis.

Hypothalamic histology

C-FOS immunohistochemistry in hypothalamus

One hour after intra-gastric gavage of sodium butyrate or vehicle, mice were anesthetized and perfused transcardially with ice-cold saline followed by freshly prepared 4% paraformaldehyde solution. The brains were collected, postfixed in 4% paraformaldehyde for 48 hours, cryoprotected in 30% sucrose and subsequently frozen on dry ice and stored at -80°C . Thirty-five μm -cryostat sections of frozen brains were cut and stored in cryoprotectant at -20°C .

c-FOS immunohistochemistry was performed on serial hypothalamic sections cut from -1.22 mm to -1.70 mm relative to the bregma according to The Mouse Brain in Stereotaxic Coordinates. Brain sections were blocked by 2% normal goat serum (NGS) and incubated with anti-c-Fos primary antibody (1:1000, Abcam), Alexa 594 secondary goat anti-rabbit antibody (1:500, Abcam) and diaminobenzidine (DAB) and DAPI as chromogen (SK-4100, Vector laboratories). The quantification of c-FOS-positive cells within the arcuate nucleus (3-4 sections per mouse) were determined using Image J software system.

Double immunofluorescent staining

Double immunofluorescent staining of c-Fos with POMC or NPY were performed on the same serial hypothalamic sections as described above. Brain sections were incubated with primary antibodies: goat anti-c-Fos (1:500, Santa Cruz), and rabbit anti-POMC (1:800, Phoenix Pharmaceuticals), or rabbit anti-NPY (1:500, Abcam), respectively, at 4°C overnight. Sections were rinsed and incubated with biotinylated secondary anti-goat or anti-rabbit IgG for 1 h, and then rinsed and incubated with streptavidin-conjugated Alexa Fluor® 594 or 647 (Jackson ImmunoResearch, USA) for 1 h. All sections were then rinsed and mounted on gelatin-coated glass slides, dried, covered with polyvinyl alcohol mounting medium containing DABCO® (Sigma, USA), observed and imaged by confocal microscopy (Leica SP8, Germany). The quantification of colocalization percentage of NPY-positive neurons or POMC-positive neurons that coexpress c-FOS within the arcuate nucleus were determined using Image J software system.

Neuron activity in brain regions of cortex, hippocampus, brainstem

c-FOS immunohistochemistry was performed on serial hypothalamic sections cut from -1.22 mm to -1.70 mm, and brainstem sections cut from -7.32 mm to -7.76 mm relative to the bregma according to The Mouse Brain in Stereotaxic Coordinates. Sections were incubated with anti-c-Fos primary antibody (1:1000, Abcam), biotinylated secondary anti-rabbit IgG, avidin-biotin complex (ABC method, Vector Laboratories, Inc., Burlingame, CA), and the reaction product was visualized by incubation in 1% diaminobenzidine with 0.01% hydrogen peroxide. The quantification of c-FOS-positive cells in cortical regions (primary somatosensory cortex and primary and secondary motor cortex), hippocampal regions, nucleus tractus solitarius (NTS) and dorsal vagal complex (DVC) within brainstem were determined using Image J software system.

Short chain fatty acid measurement by the gas chromatography–mass spectrometry (GC-MS)

Plasma short chain fatty acids were analysed by GC-MS using previously published approach with some modifications¹. Briefly, 10 μ L of plasma was transferred to a glass vial containing 250 μ L acetone (Sigma-Aldrich), 10 μ L 1 ppm internal standards solution containing acetic acid-d₄, propionic acid-d₆ and butyric acid-d₈ (Sigma Aldrich) and 10 μ L ethanol. Thereafter, samples were derivatized with pentafluorobenzyl bromide (PFBBBr), as follows: 100 μ L 172 mM PFBBBr (Thermo) in acetone was added, samples were mixed and heated to 60 °C for 30 min. After the samples had cooled down to room temperature a liquid-liquid extraction was performed using 500 μ L n-hexane (Sigma-Aldrich) and 250 μ L GC-MS grade water. The upper n-hexane layer was transferred to a fresh glass vial and subsequently used for GC-MS analysis. Calibration standards were prepared analogous. For calibration standards no plasma was added and 10 μ L of EtOH was replaced by 10 μ L standards solution (Sigma-Aldrich) in EtOH.

Samples were analysed on a Bruker Scion 436 GC fitted with an Agilent VF-5ms capillary column (25m \times 0.25mm i.d., 0.25 μ m film thickness) coupled to a Bruker Scion TQ MS. Injection was performed using a CTC PAL autosampler (G6501-CTC): 1 μ L sample was injected splitless at 280 °C. Helium 99.9990% was used as carrier gas at a constant flow of 1.20 mL/min. The GC temperature program was set as follows: 1 min. constant at 50 °C, then linear increase at 40 °C/min. to 60 °C, kept constant for 3 min., followed by a linear increase at 25 °C/min to 200 °C, linearly increased at 40 °C/min to 315 °C, kept constant for 2 min.. The transfer line and ionization source temperature were 280 °C. The pressure of the chemical ionization gas, methane (99.9990%), was set at 15 psi. Negatively charged ions were detected in the selected ion monitoring mode, and acetic acid, acetic acid-d₄, propionic acid, propionic acid-d₆, butyric acid and butyric acid-d₈ were monitored at m/z 59, 62, 73, 78, 87 and 94 respectively.

Body weight and body composition

Body weight was measured with a scale, and body composition was measured in conscious mice using an EchoMRI-100 analyzer (EchoMRI, Houston, TX).

Hepatic lipid content

Liver lipids were extracted according to a modified protocol from Bligh and Dyer². Small liver pieces (approx. 30 mg) were homogenized in ice-cold methanol. By addition of CH₃OH:CHCl₃ (1:3 v/v) to the homogenate, followed by vigorous vortexing and phase separation by centrifugation, lipids were extracted into the CHCl₃ phase. Subsequently, the lipid phase was dried and dissolved in 2% Triton X-100. TG, total cholesterol (TC) and phospholipid (PL) concentrations were measured using the commercial kits 11488872, 236691 (Roche Molecular Biochemicals) and phospholipids B (Wako Chemicals), respectively. Hepatic lipid content was expressed as nmol lipid per mg protein, which was determined using the BCA protein assay kit (Pierce).

Plasma parameters

After a 5-h fasting period (8am-1pm), blood was obtained via tail vein bleeding into heparin-coated capillary tubes just before the sodium butyrate supplementation and at the end of the intervention. The capillary tubes were placed on ice and centrifuged, and obtained plasma was snap-frozen in liquid nitrogen and stored at -80°C until further measurements. Plasma was assayed for TG, glucose and insulin using commercially available kits as described previously³. The homeostasis model index of insulin (HOMA-IR) as an index for insulin resistance was calculated by multiplying fasting insulin (mU/L) with fasting glucose (nmol/L), and dividing by 22.5⁴.

In vivo lipid and glucose clearance

Triacylglycerol-rich lipoprotein (TRL)-like particles (average size of 80 nm) labeled with glycerol tri[³H]oleate (triolein, [³H]TO) were prepared and mixed with 2-[1-¹⁴C]deoxy-D-glucose ([¹⁴C]DG) in a 3:1 ratio based on radioactive counts. Particles were stored at 4°C under argon and used for *in vivo* kinetic experiments.

At 9.00 am, mice were injected with 200 µL of emulsion particles (1 mg TG) and [¹⁴C]DG via the tail vein at the end of the intervention period. Blood samples were taken at 2, 5, 10 and 15 min after injection, and lipid and glucose clearance kinetics were determined by measuring plasma ³H and ¹⁴C activities. After 15 min, mice were sacrificed by cervical dislocation and perfused with ice-cold saline via the heart. Thereafter, organs were harvested and weighed and dissolved overnight at 60°C in a Tissue Solubilizer (Amersham Biosciences, Roosendaal, the Netherlands). The uptake of [³H]TO- and [¹⁴C]DG-derived radioactivity by the organs was calculated from the ³H and ¹⁴C activities in each organ and expressed as percentage of injected dose per gram wet tissue weight.

Indirect calorimetry

Indirect calorimetry was performed in fully automatic metabolic cages (LabMaster System, TSE Systems, Bad Homburg, Germany) in the first week of the intervention. After 2 days of acclimatization, O₂ consumption, CO₂ production and physical activity were measured for 3 consecutive days. The

average respiratory exchange ratio, energy expenditure, fat and carbohydrate oxidation rates were calculated as described previously.⁵

BAT histology and TG content

Formalin-fixed paraffin-embedded interscapular BAT (iBAT) tissue sections (5 μm) were prepared for haematoxylin and eosin (H&E) staining using standard protocols, and stained for uncoupling protein-1 (UCP-1, 1/4000; Ab10983; Abcam) and tyrosine hydroxylase (TH, 1/2000; Ab112; Abcam) as described previously⁶. The areas occupied by intracellular lipid vacuoles, nuclear, UCP-1 and TH were quantified using Image J software (National Institutes of Health). The protein content of UCP-1 was expressed as positive area per total iBAT area, and the protein content of TH was expressed as positive area per cell nuclear area, which was represented the cell number.

WAT histology and adipocyte size

Formalin-fixed paraffin-embedded subcutaneous WAT (sWAT) and gonadal WAT (gWAT) sections (5 μm) were prepared for haematoxylin and eosin (H&E) staining using standard protocols, and stained for uncoupling protein-1 (UCP-1, 1/4000; Ab10983; Abcam). The average adipocyte size (μm^2) was quantified per mouse using Image J software (National Institutes of Health), and normalized to Control group.

Microbiota analysis

After 7 weeks of butyrate treatment, total cecal bacterial DNA was isolated from cecum content in mice received subdiaphragmatic vagotomy surgery or sham surgery as described previously⁷. Microbial 16S rRNA gene was amplified targeting the hyper-variable region V4. Sequencing was performed using the Illumina MiSeq platform (BGI Genomics, Hong Kong) generating paired-end reads of 250 bp in length in each direction. Overlapping paired-end reads were subsequently aligned. Reads quality was checked with Sickle, version:1.33 (<https://github.com/najoshi/sickle>) and low quality reads were removed. For visualising the taxonomic composition of the fecal microbiota and further beta diversity analysis, QIIME version: 1.9.1 was used⁸. In brief, closed reference operational taxonomic unit (OTU) picking with 97% sequence similarity against GreenGenes 13.8 reference database was done. Jackknifed beta-diversity of unweighted UniFrac distances with 10 jackknife replicates was measured at rarefaction depth of 20000 reads /sample. For statistical significance, biological relevance and visualisation we used linear discriminant analysis (LDA) effect size (LEfSe) method which uses standard parameters ($P < 0.05$ and LDA score 2.0) as described in (<https://bitbucket.org/biobakery/biobakery/wiki/lefse>).

SUPPLEMENTAL TABLES AND FIGURES

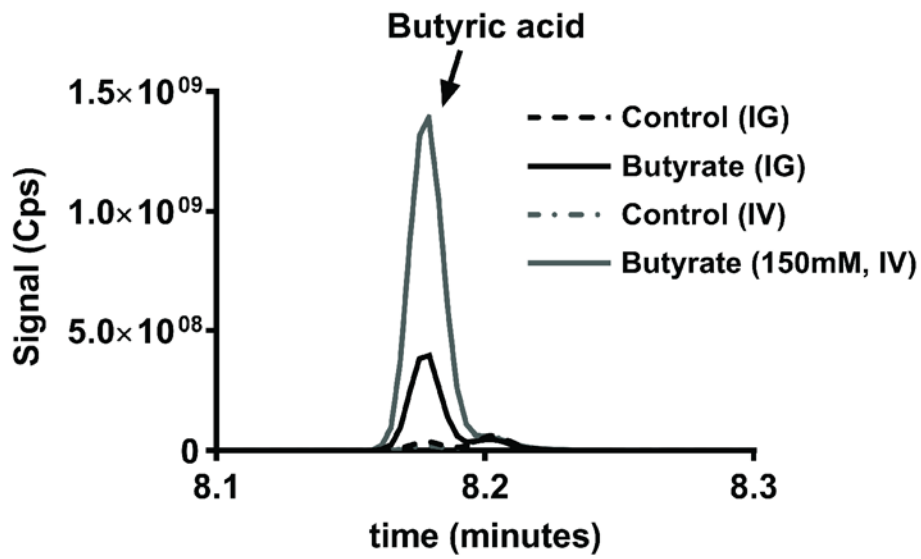


Figure S1. Oral and intravenous butyrate supplementation increases plasma butyrate concentration

After overnight fasting and randomization based on bodyweight, mice received vehicle or butyrate via the intra-gastric gavage (IG) or intravenous injection (IV). 1 hour after receiving butyrate, plasma were pooled for the measurement of butyrate level by GC-MS.

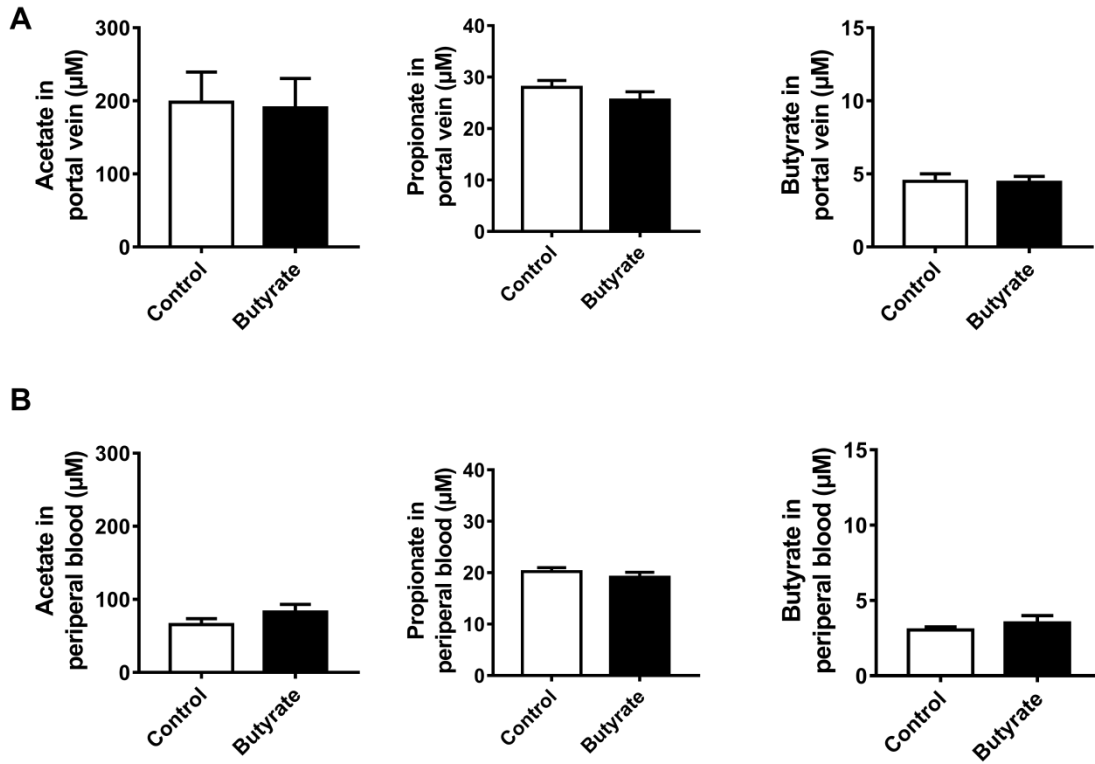


Figure S2. Chronic dietary butyrate consumption does not alter the levels of acetate, propionate and butyrate in portal vein or peripheral blood

Mice were individually housed and receive a HFD without (Control group), or with 5% (w/w) sodium butyrate (Butyrate group) for 9 weeks. At the end of this study, portal vein blood and peripheral blood were collected, the levels of acetate, propionate and butyrate were determined by GC-MS. Data are means \pm SEM (n=6-7).

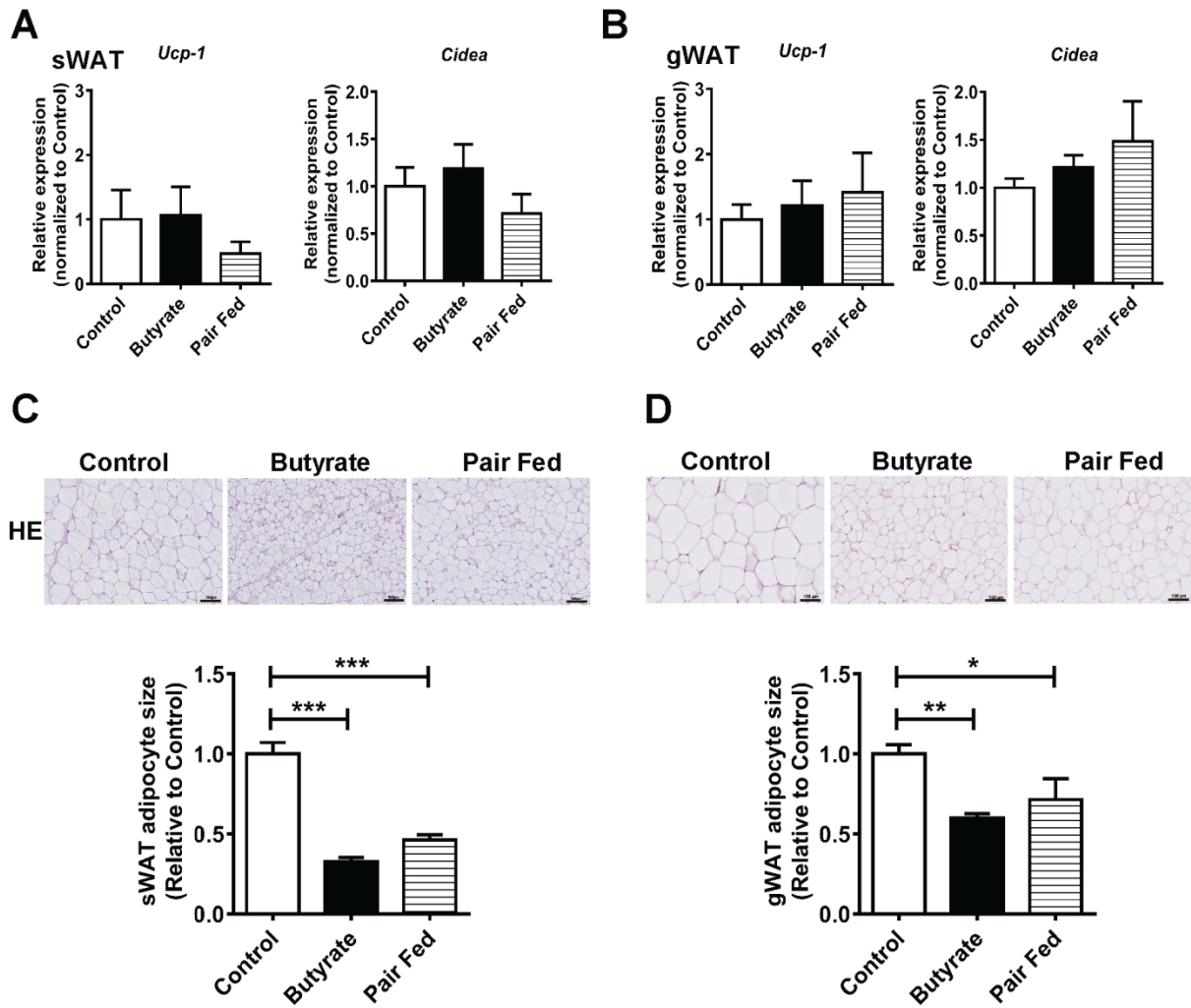


Figure S3. Butyrate treatment does not induce browning of white adipose tissue

After 9 weeks of intervention, the subcutaneous white adipose tissue (sWAT, A,C) and gonadal white adipose tissue (gWAT, B,D) were collected. mRNA expression of *Ucp-1* and *Cidea* were determined (A, B). Slides were stained for H&E, and the adipocyte size was quantified (C, D). Data are means \pm SEM (n=8-9). *P<0.05, **P<0.01, ***P<0.001 as compared to control group.

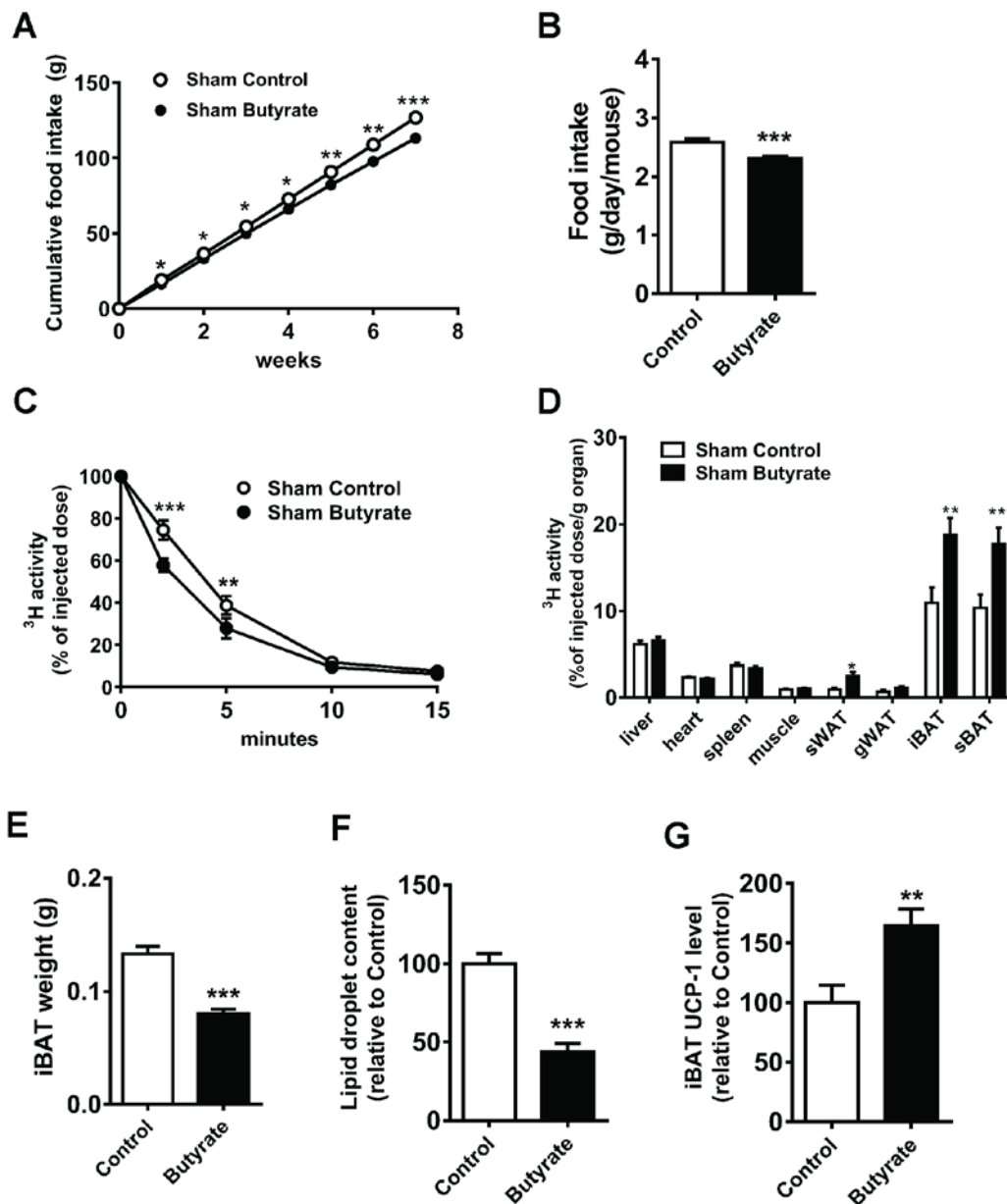


Figure S4. Butyrate decreases food intake and activates brown adipose tissue in mice received sham surgery (related to Figure 6)

Mice were individually housed and received sham surgery. One week after the surgery, mice were fed a HFD without (Sham Control) or with 5% (w/w) sodium butyrate (Sham Butyrate) for 7 weeks. Food intake was measured weekly and cumulative food intake (A) and average food intake *per se* (B) was calculated. At the end of this study, a TG clearance test by i.v. injection of [³H]TO-labeled TRL-like particles was performed. The clearance of [³H]TO from the circulation (C) and uptake of ³H by various tissue (D) was assessed. The weight of iBAT pad (E) was measured and the lipid content within the iBAT was quantified after the H&E staining (F). The protein expression of UCP-1 in iBAT was quantified after IHC of UCP-1 (G). Data are means ± SEM (n=8-9); *P<0.05, **P<0.01, ***P<0.001 compared to sham control.

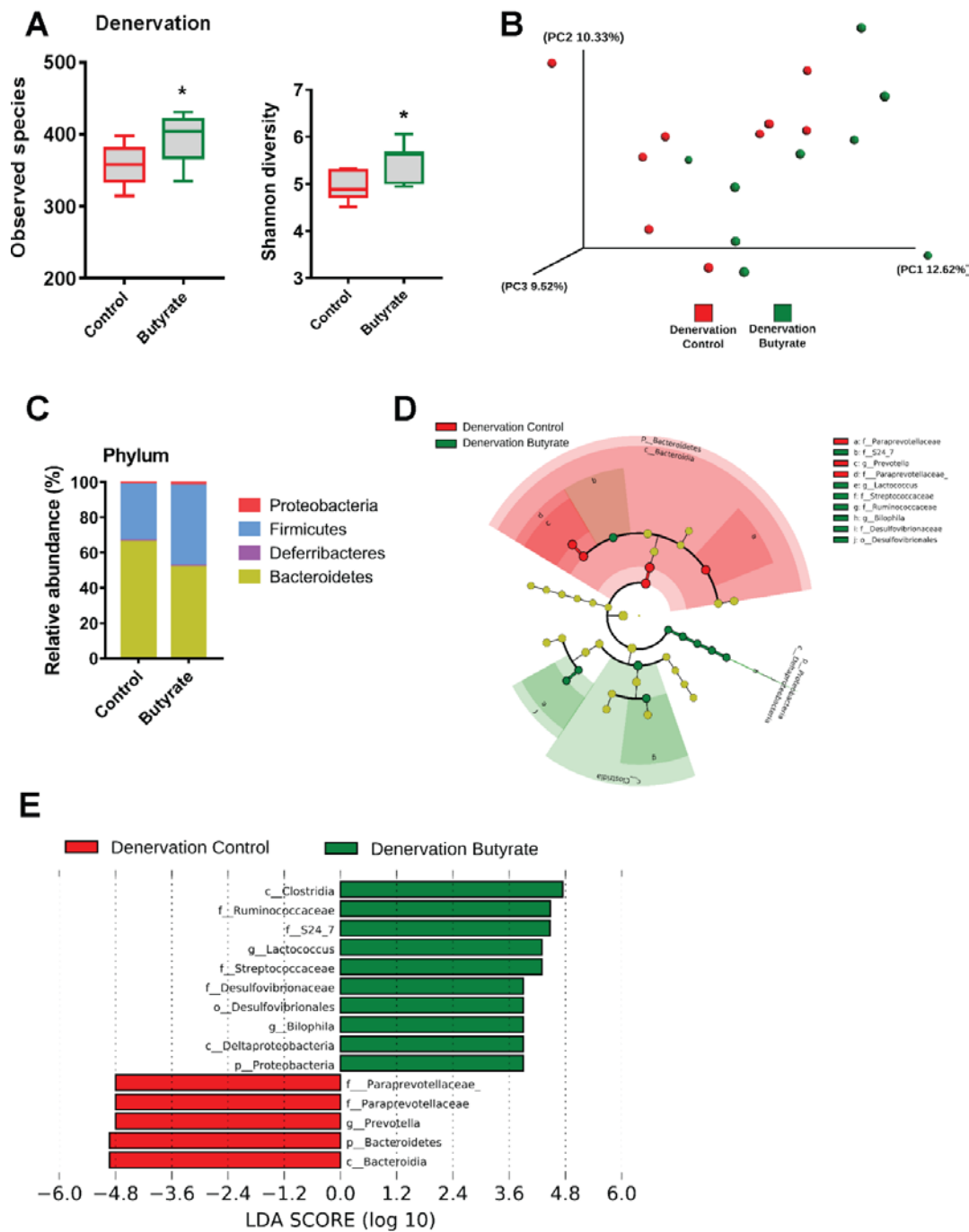


Figure S5. Butyrate consumption alters gut microbiota composition

After 7 weeks of intervention, total cecal bacterial DNA was isolated from the cecum content in mice received subdiaphragmatic vagotomy surgery and 16S rRNA genes were sequenced. (A) The α diversity including observed species and Shannon diversity of the gut microbiota. (B) Principal coordinates analysis plot of Unweighted Unifrac distances. Composition of abundant bacterial phyla (C), Cladogram generated from LEfSe analysis (D) and the LDA score (E) showing the most differentially significant abundant taxa enriched in microbiota from the denervation control (red) and denervation butyrate (green) group. For A, data was shown as Box& whiskers, Mann-Whitney test, * $P < 0.05$ as compared to denervation control group.

Reference List

- (1) Tomcik K, Ibarra RA, Sadhukhan S, Han Y, Tochtrop GP, Zhang GF. Isotopomer enrichment assay for very short chain fatty acids and its metabolic applications. *Anal Biochem* 2011 March 1;410(1):110-7.
- (2) BLIGH EG, DYER WJ. A rapid method of total lipid extraction and purification. *Can J Biochem Physiol* 1959 August;37(8):911-7.
- (3) Wang Y, Parlevliet ET, Geerling JJ, van der Tuin SJ, Zhang H, Bieghs V, Jawad AH, Shiri-Sverdlov R, Bot I, de Jager SC, Havekes LM, Romijn JA, Willems van DK, Rensen PC. Exendin-4 decreases liver inflammation and atherosclerosis development simultaneously by reducing macrophage infiltration. *Br J Pharmacol* 2014 February;171(3):723-34.
- (4) Mather K. Surrogate measures of insulin resistance: of rats, mice, and men. *Am J Physiol Endocrinol Metab* 2009 February;296(2):E398-E399.
- (5) Van Klinken JB, van den Berg SA, Havekes LM, Willems van DK. Estimation of activity related energy expenditure and resting metabolic rate in freely moving mice from indirect calorimetry data. *PLoS One* 2012;7(5):e36162.
- (6) Kooijman S, Wang Y, Parlevliet ET, Boon MR, Edelschaap D, Snaterse G, Pijl H, Romijn JA, Rensen PC. Central GLP-1 receptor signalling accelerates plasma clearance of triacylglycerol and glucose by activating brown adipose tissue in mice. *Diabetologia* 2015 November;58(11):2637-46.
- (7) Janssen AWF, Houben T, Katiraei S, Dijk W, Boutens L, van der Bolt N, Wang Z, Brown JM, Hazen SL, Mandard S, Shiri-Sverdlov R, Kuipers F, Willems van DK, Vervoort J, Stienstra R, Hooiveld GJEJ, Kersten S. Modulation of the gut microbiota impacts nonalcoholic fatty liver disease: a potential role for bile acids. *J Lipid Res* 2017 July;58(7):1399-416.
- (8) Caporaso JG, Kuczynski J, Stombaugh J, Bittinger K, Bushman FD, Costello EK, Fierer N, Pena AG, Goodrich JK, Gordon JI, Huttley GA, Kelley ST, Knights D, Koenig JE, Ley RE, Lozupone CA, McDonald D, Muegge BD, Pirrung M, Reeder J, Sevinsky JR, Turnbaugh PJ, Walters WA, Widmann J, Yatsunenko T, Zaneveld J, Knight R. QIIME allows analysis of high-throughput community sequencing data. *Nat Methods* 2010 May;7(5):335-6.